Measurement report: Brown Carbon Aerosol in Polluted Urban Air of North China Plain: Day-night Differences in the Chromophores and Optical Properties

Yuquan Gong[1,2], Ru-Jin Huang[1,2,3,~~4~~], Lu Yang[1,2], Ting Wang[1], Wei Yuan[1,2], Wei Xu[1], Wenjuan Cao[1], Yang Wang[~~4,~~5,~~6~~], Yongjie Li[~~6~~7]

[1]State Key Laboratory of Loess and Quaternary Geology, CAS Center for Excellence in Quaternary Science and Global Change, Institute of Earth Environment, Chinese Academy of Sciences, 710061 Xi'an, China

[2] University of Chinese Academy of Sciences, Beijing 100049, China

[3] Institute of Global Environmental Change, Xi'an Jiaotong University, Xi'an 710049, China

~~[4] Laoshan Laboratory, Qingdao 266061, China~~

[~~4~~5] School of Geographical Sciences, Hebei Normal University, Shijiazhuang, China

[~~5~~6] State Key Joint Laboratory of Environmental Simulation and Pollution Control, Beijing, China

[~~6~~7] Department of Civil and Environmental Engineering, Faculty of Science and Technology, University of Macau, Taipa, Macau SAR 999078, China

Correspondence: E-mail: rujin.huang@ieecas.cn (R.-J.H)

Abstract. Brown carbon (BrC) aerosol is light-absorbing organic carbon that affects radiative forcing and atmospheric photochemistry. The BrC chromophoric composition and its linkage to optical properties at the molecular level, however, are still not well characterized. In this study, we investigate the day-night differences in the chromophoric composition (38 species) and optical properties of water-soluble and water-insoluble BrC fractions (WS-BrC and WIS-BrC) in aerosol samples collected in Shijiazhuang, one of the most polluted cities in China. We found that the light absorption contribution of WS-BrC to total BrC at 365 nm was higher during the day (62 ± 8%) than during the night (47 ± 26%), which is in line with the difference in chromophoric polarity between daytime (more polar nitrated aromatics) and nighttime (more less-polar polycyclic aromatic hydrocarbons, PAHs). The high polarity and water solubility of BrC in daytime suggests the enhanced contribution of secondary formation to BrC during the day. There was a decrease of the mass absorption efficiency of BrC from nighttime to daytime (2.88 ± 0.24 vs. 2.58 ± 0.14 for WS-BrC and 1.43 ± 0.83 vs. 1.02 ± 0.49 m^2 g C^{-1} for WIS-BrC, respectively). Large polycyclic aromatic hydrocarbons (PAHs) with 4–6-rings PAHs and nitrophenols contributed to 76.7% of the total light absorption between 300–420 nm at night time, while nitrocatechols and 2–3-ring oxygenated PAHs accounted for 52.6% of the total light absorption at day. The total mass concentrations of the identified chromophores showed larger day-night difference during the low-pollution period (day-to-night ratio of 4.3) than during the high-pollution period (day-to-night ratio of 1.8). The large day-night difference in BrC composition and absorption, therefore, should be considered when estimating the sources, atmospheric processes and impacts of BrC.

1 Introduction

Light-absorbing organic carbon aerosols, also termed brown carbon (BrC) aerosol, are ubiquitous in the atmosphere (Iinuma et al., 2010; Yuan et al., 2016; Huang et al., 2021). Growing evidence has shown that BrC can reduce atmospheric visibility, affect atmospheric photochemistry, and change regional and global radiation balance (Kirchstetter et al., 2004; Laskin et al., 2015; Hammer et al., 2016). Besides, some components in BrC, such as polycyclic aromatic hydrocarbons (PAHs) are highly toxic and carcinogenic, which can adversely impact human health (Alcanzare, 2006; Zhang et al., 2009; Huang et al., 2014). The extent of these effects is closely related to the optical properties and chemical composition of BrC, which are still not well understood.

BrC is often classified into water-soluble (WS-BrC) and water-insoluble (WIS-BrC) fractions because these two fractions are largely different in chemical composition and light absorption. For example, abundant nitrophenols were detected in WS-BrC, while polycyclic aromatic hydrocarbons (PAHs) were the main component of WIS-BrC (Huang et al., 2018; Huang et al., 2020). The difference in BrC chemical composition is associated with the emission sources. For example, methyl nitrocatechols are specific to biomass burning, while PAHs are mainly emitted by fossil fuel combustion (Kitanovski et al., 2012; Dat and Chang, 2017). Atmospheric oxidation can further complicate the BrC chromophores dynamically, leading to light-absorbing enhancement or bleaching. For example, Li et al. (2020) reported that the mass absorption efficient (MAE) of some nitroaromatic compounds (e.g., nitrocatechols) from the biomass burning can enhance about 2−3 times by oxidation to generate secondary chromophores. Yet, prolonged photo-oxidation reactions (exposure to sunlight for few hours) of these nitroaromatic can generate small fragment molecules (e.g., malonic acid, glyoxylic acid) and rapidly reduce the particle absorption (Hems and Abbatt, 2018; Wang et al., 2019b; Li et al., 2020). The complexity in composition and sources, as well as the dynamics in their atmospheric processing limit our understanding in BrC chromophores and their links to light absorption.

In recent years, a growing number of studies have investigated the chromophore composition of BrC and found that nitro-phenols, low ring acids/alcohols, PAHs and carbonyl

oxygenated PAHs (OPAHs) were the major chromophores in BrC (Teich et al., 2017; Yuan et al., 2020; Huang et al., 2020). Some chromophores in BrC can be generated from both primary emission and secondary formation. For example, 4-nitrophenol and 4-nitrocatechol can be emitted directly from biomass burning and can also be generated through photo-oxidation reactions (Kitanovski et al., 2012; Yuan et al., 2020). The differences in emission sources or atmospheric oxidation conditions have a significant effect on the chemical composition of BrC chromophores. Previous studies mainly focused on seasonal variations of BrC chromophores (Wang et al., 2018; Kasthuriarachchi et al., 2020; Yuan et al., 2021), and the diurnal variation of WS-BrC in fluorescence and inorganic fractions (Deng et al., 2022; Zhan et al., 2022), however, the research of BrC chemical composition on day-night differences is scarce. In this study, the optical properties and chemical composition of the WS-BrC and WIS-BrC in daytime and nighttime were measured with a high-performance liquid chromatography–photodiode array–high-resolution mass spectrometry platform (HPLC-PDA-HRMS) in $PM_{2.5}$ samples collected in Shijiazhuang, one of the most polluted cities in the Beijing-Tianjin-Hebei region. Besides, the relationship between the concentration and light-absorbing contributions of the BrC subgroups was analyzed. The object of this study is to investigate the day-night differences in the optical properties and chromophore composition of BrC and to explore the effect of primary emissions and atmospheric processes on the light absorption and chemical composition of BrC.

2 Experimental

2.1 Sample collection.

Day and night $PM_{2.5}$ samples were collected on the quartz-fiber filters (8*10 in., Whatman, QM-A; filters prebaked at 750 °C, over 3 h) through a high-volume air sampler (Hi-Vol $PM_{2.5}$ sampler, Tisch, the velocity of flow ~1.03 m^3 min^{-1}, Cleveland, OH) from 17 January to 13 February 2014. Daytime samples were collected from 08:30 to 18:30 (~10 hours), and nighttime samples are collected from 18:30 to the next day at 8:30 (~14 hours). After collection, the samples were stored in a freezer (-20°C) until analysis. The sampling site was located on the rooftop of a building (~15 m above ground) in the Institute of Genetics and Developmental

Biology, Chinese Academy of Sciences (38.2° N, 114.3° E), which is surrounded by a residential–business mixed zone.

2.2 Light Absorption Measurement.

A portion filter (about 0.526 cm^2 punch) was taken from collected samples and sonicated for 30 min in 10 mL of ultrapure water (>18.2 MΩ) or methanol (J. T. Baker, HPLC grade), and then the extracts WS-BrC and methanol soluble BrC (MS-BrC) were obtained. The extracts were filtered with a 0.45 μm PVDF (water soluble) or PTFE (water insoluble) pore syringe filter to remove insoluble substances. The light absorption spectra of the filtrate were tested using a UV-VIS spectrophotometer (Ocean Optics) over the range from 250 nm to 700 nm, equipped with a liquid waveguide capillary cell (LWCC-3100, World Precision Instruments, Sarasota, FL, USA), following the method of Hecobian et al. (2010). To ensure reliable absorbance measurements (Absorbance between 0.2 to 0.8 at 300 nm in this study), the filtrate was diluted with appropriate folds before absorption spectra measurements. In this study, the light-absorbing of WIS-BrC is obtained by MS-BrC minus WS-BrC. As shown in Figure S1~~3~~, the summed absorbance of WS-BrC and WIS-BrC is very close to the absorbance of MS-BrC (difference less than 5%). Therefore, the interferences of solvent and pH on the measurement of WIS-BrC should be very limited. The pH of the water extracts was not adjusted because highly diluted water extracts was used to measure the light absorption, and little change of pH was observed for water extracts of different samples. The light absorption coefficient (Abs) and absorption data were calculated following the equation:

$$Abs_\lambda = (A_\lambda - A_{700})\frac{V_l}{V_b \times l} \times \ln(10)$$

where Abs_λ ($M\text{-}m^{-1}$) represents the sample absorption coefficient at wavelength of λ; A_λ is the absorbance recorded (Random wavelength); A_{700} for explaining baseline drift as the reference during data analysis. To account for baseline drift that may occur during analysis, absorption at all wavelengths below 700 nm are referenced to that at 700 nm where there is no absorption for BrC extracts. V_l (ml) is the total volume of solvent (water or methanol) used to extract the quartz-fiber filters; V_b (m^3) represents the volume of through the filter sample of the air; l (0.94 m) is the optical path length of UV-VIS spectrophotometer and ln (10) is the absorption coefficient with base-e, which is the natural logarithm by using the logarithm conversion with

the base-10.

About the mass absorption efficiency (MAE) of the filter extracts at wavelength of λ can be defined as:

$$MAE_\lambda = Abs_\lambda / C_{OM}$$

where C_{OM} (μg m^{-3}) stands for the concentration of water-soluble organic carbon (WSOC) or methanol extracts methanol-soluble organic carbon (MSOC). The concentrations of WSOC were measured with a TOC-TN analyzer (TOC-L, Shimadzu, Japan). The concentration of OC was measured by a thermal-optical carbon analyzer (DRI, Model 2001) with the IMPROVE A protocol (Chow et al., 2011). Note that MSOC is usually replaced with OC because previous studies have shown that methanol has a high extraction efficiency (~90%) for OC. But it is difficult to completely extract the OC by methanol (Chen and Bond, 2010; Cheng et al., 2016; Xie et al., 2019). Here, WISOC is obtained by MSOC minus WSOC.

The wavelength dependence that the light absorption chromophore of solution can be characterized by this equation:

$$Abs_\lambda = K \cdot \lambda^{-AAE}$$

where K is the fitting parameter of the extracts which is constant related to the chromophoric concentration; AAE is known as the absorption Ångström exponent, which depends on the types of chromophores in the solution. In this study, AAE was calculated by linear regression of $\log_{10}$ Abs $_\lambda$ versus $\log 10_\lambda$ at 300–400 nm.

The MAE of standards samples ($MAE_{S,\lambda}$), e.g., 4-nitrocatechol and 4-nitrophenol, in the water or methanol solvent at a wavelength of λ were calculated as the Laskin et al. (2015)

$$MAE_{S,\lambda} = \frac{A_\lambda - A_{700}}{l \times C} \ln(10)$$

where C (μg mL^{-1}) is the concentration of the standards in the extracts.

2.3 BrC Chemical composition analysis.

The main chromophores in WS-BrC and WIS-BrC were identified by the HPLC-PDA-HRMS platform (Thermo Electron, Inc.), and the details are presented in our previous study (Huang et al., 2020). Firstly, the filter samples (3.5~48.3 cm^2) were ultrasonically extracted with 6 mL of the ultrapure water for 30 min and repeated two times. The extracts were filtered through a PVDF filter (0.45 μm) to remove insoluble materials. Then the solution was subjected

to an SPE cartridge (Oasis HLB, USA) to remove water-soluble inorganic salt ions. On the other hand, the residual filters were dried and the WIS-BrC fractions were further extracted two times with 6 mL of methanol for 30 min. to extract the WIS-BrC fractions. Afterward, the extracts of WS-BrC and WIS-BrC chromophores were dried with a gentle stream of nitrogen and then redissolved in 150 μl of ultrapure water and methanol.

The BrC factions were analyzed by an HPLC-PDA-HRMS platform (including the Dionex UltiMate system and the high-resolution Q Exactive Plus hybrid quadrupole-Orbitrap mass spectrometer). Here, the extracts were loaded onto a Thermo Accucore RP-MS column by the binary solvent with an aqueous solution containing 0.1% formic acid and methanol solution containing 0.1% formic acid as mobile phases L_1 and L_2, eluting at a flow rate of 0.3 mL min^{-1}. The process of gradient elution here was set as follows: firstly, aggrandize linearly the concentration of L_2 from 15% to 30% in the preliminary 15 minutes, and then linearly increased to 90% from 15 to 45minutes, held at 90% from 45 to 50 minutes, afterward decreased to 15% from 50 to 52 minutes and held there for 60 minutes. The Q Exactive Plus hybrid quadrupole-Orbitrap mass spectrometer, negative/positive mode ESI (-)/ESI (+) for details usage and data processing can refer to in the article by Huang et al. (2020) and Liu et al. (2016). Briefly, HPLC/PDA/HRMS platform was employed in ESI (-) and ESI (+) mode to acquire BrC fractions that mass range from m/z 100 to 800. Strongly polar aromatic hydrocarbons like nitrophenol and carboxylic acid are preferentially ionized in ESI (-) mode~~, conversely, ESI (+) mode is helpful to detect oxygenated aliphatic compounds and nitrogen bases OPAHs (Oxygenated PAHs) and PAHs fractions~~ (Lin et al., 2017). OPAHs and nitrogen heterocyclic PAHs were quantified in ESI (+) mode, while PAHs were detected by PDA spectroscopic analysis due to their super low ionization efficiency in ESI. The absorption spectra of chromophores were measured by a PDA detector in the wavelength range of 190-700 nm. The results of this study were corrected by a blank.

The elemental composition of individual chromatographic peaks was assigned with the molecular formula calculator in Xcalibur 4.0 software using a mass tolerance of ±3 ppm and the maximum numbers of atoms for the formula calculator were set as 30 ^{12}C, 60 ^{1}H, 15 ^{16}O, 3 ^{14}N, 1 ^{32}S, 1 ^{23}Na. To eliminate the chemically unreasonable formulas, the identified formulas

were constrained by setting 0.3 ≤ H/C ≤ 3.0, 0.0 ≤ O/C ≤ 3.0, 0.0 ≤N/C ≤ 0.5, 0.0 ≤ S/C ≤ 0.2 in ESI- mode and 0.3 ≤ H/C ≤ 3.0, 0.0 ≤ O/C ≤ 3.0, 0.0 ≤N/C ≤ 1.3, 0.0 ≤ S/C ≤ 0.8 in ESI+ mode, as suggested in a previous study (Lin et al., 2012). Further, the calculated neutral molecular formulas that did not fit the nitrogen rule were excluded. In total, 20 WS-BrC chromophores (two quinolines, four 2-3 ring OPAHs, four nitrocatechols, six nitrophenols and four aromatic alcohols & acids) and 18 WIS-BrC chromophores (three 4-ring OPAHs and 15 PAHs) were identified and their concentrations were quantified with authentic standards (28 species) or surrogates (10 species) (see Table S1). Thereinto, the WS-BrC chromophores, benzanthrone (21#) and benzo[b]fluoren-11-one (22#) were quantified by mass spectrometry analysis in either negative or positive ESI mode, while the rest of WIS-BrC chromophores were quantified by PDA spectroscopic analysis due to their super low ionization efficiency in ESI (see Table S1).~~In this study, 38 BrC components (20 WS-BrC and 18 WIS-BrC species) were detected by mass spectrometry and PDA spectroscopy (see Table S1). Thereinto, the main absorbing chromophores in ambient aerosol samples (28 species) were identified by standards. Of course, some BrC chromophores that cannot be accurately identified (substances with (*), see Table S1 in Supplemental Information), we will select the more reasonable structure from those that satisfy the molecular weight, the ratios of CcHhOoNnSsNax (setting 0.3 ≤ H/C ≤ 3.0, 0.0 ≤ O/C ≤ 3.0, 0.0 ≤N/C ≤ 0.5, 0.0 ≤ S/C ≤ 0.2.), the double bond equivalent (DBE/C ≥ 0.5), and polarity (water soluble/water in-soluble) (Huang et al., 2020). Mass data processed by the Xcalibur 4.0 software which the parameter of molecular mass set in ± 3 ppm and maximum numbers of atoms for the formula calculator set as 30 ^{12}C, 60 ^{1}H, 15 ^{16}O, 3 ^{14}N, 1 ^{32}S, 1 ^{23}Na. The results of this study were corrected by a blank.~~

3 Results and discussion

3.1 Optical properties of BrC during the day and night.

Figure 1 (a) shows the average absorption spectra of WS-BrC and WIS-BrC at the wavelength range between 300 and 500 nm during the day and the night. It can be seen that the light absorption of both WS-BrC and WIS-BrC sharply increased toward the short wavelength. The average absorbance of WS-BrC is 46.04 ± 35.92 Mm^{-1} (at 365 nm) during the day that is

higher than the night (35.68 ± 35.50 Mm^{-1}). However, the light absorption of WIS-BrC at 365 nm is much lower during the night (27.90 ± 24.80 Mm^{-1}) than during the day (40.89 ± 23.42 Mm^{-1}). The day-night differences of light absorption of WS-BrC and WIS-BrC indicates the difference in water solubility and polarity of the chromophores. The average AAE of WS-BrC ($AAE_{WS\text{-}BrC}$) and WIS-BrC ($AAE_{WIS\text{-}BrC}$) during the day are 5.10 ± 0.28 and 6.36 ± 0.45, respectively, which are lower than those of the night (5.51 ± 0.40 and 6.97 ± 0.80, respectively). Note that both during the day and night the $AAE_{WS\text{-}BrC}$ is lower than $AAE_{WIS\text{-}BrC}$, which is different from findings in previous studies (see Table S2). For example, Huang et al. (2020) found that the $AAE_{WS\text{-}BrC}$ was higher (8.2 ± 1.0 and 8.2 ± 1.0 in Beijing and Xi'an, respectively) than that of $AAE_{WIS\text{-}BrC}$ (5.7 ± 0.2 and 5.4 ± 0.2 in Beijing and Xi'an, respectively). Besides, MAE_{365} of WS-BrC are 2.0- and 2.5-fold of WIS-BrC during the day (2.88 ± 0.24 vs. 1.43 ± 0.83 $m^2\ g\ C^{-1}$) and night (2.58 ± 0.14 vs. 1.02 ± 0.49 $m^2\ g\ C^{-1}$), respectively, which is opposed to the results of previous studies. For example, the MAE_{365} of WS-BrC are 0.7- and 0.5-fold of WIS-BrC in winter of Beijing (1.22 ± 0.11 vs. 1.66 ± 0.48 $m^2\ g\ C^{-1}$) (Chen and Bond, 2010) and Xi'an (1.00 ± 0.18 vs. 1.82 ± 1.06 $m^2\ g\ C^{-1}$) (Li et al., 2020), respectively. This result indicates that the chemical composition of BrC in the most polluted city, Shijiazhuang, is different from other urban areas on primary sources and secondary aging process. However, both WS-BrC and WIS-BrC have higher MAE_{365} and average AAE values during the day than the night. This suggests that the day-night differences of AAE and MAE_{365} of BrC fractions are likely associated with the different primary emissions and atmospheric aging processes (Cheng et al., 2016; Wang et al., 2019a; Wang et al., 2020). For example, the AAE and MAE_{365} of BrC emitted from biomass burning (AAE ~7.31, and MAE_{365} ~1.01 $m^2\ g\ C^{-1}$, respectively) (Siemens et al., 2022) showed large differences with that from vehicle emissions (AAE ~10.5, and MAE_{365} ~0.32 $m^2\ g\ C^{-1}$) (Xue et al., 2018). Besides, photochemical oxidation of fresh BrC from coal combustion resulted in considerable changes in AAE and MAE_{365}, e.g., the AAE and MAE_{365} of fresh coal combustion emission are 7.2 and 0. 84 ± 0.54 $m^2\ g\ C^{-1}$, much higher than those in aged samples (6.4 and 0.14 ± 0.08 $m^2\ g\ C^{-1}$, respectively) (Ni et al., 2021).

Figure 1 (b) shows the light absorption contributions of WS-BrC and WIS-BrC to total BrC over the wavelength range of 300–500 nm. It is obvious that the absorption contribution

of WS-BrC is increased from 53.8% at 300 nm to 87.4% at 500 nm during the day, and from 38.4% to 61.5% during the night. The higher absorption contributions of WS-BrC at longer wavelengths during the day compared to that of the night may be related to photo-oxidation reaction in day time (Wang et al., 2019b; Chen et al., 2021). The absorption contribution of WS-BrC accounts for 62 ± 8% to total BrC absorption at 365 nm during the day, but only 47 ± 8% during the night. The large difference in BrC light absorption between samples from the day and those from the night observed in this study is comparable with previous studies (Shen et al., 2019; Li et al., 2020), and indicates the significant day-night difference in chemical composition.

3.2 Composition and absorption contribution of BrC during day and night.

In total, 38 major chromophores were quantified in WS-BrC and WIS-BrC with HPLC-PDA-HRMS analysis, and the concentrations of these chromophores are shown in Table S3. According to the characteristics of the molecular structures and absorption spectra, these chromophores are divided into ten subgroups, including two quinolines, four nitrocatechols, six nitrophenols, four aromatic alcohols/acids, four 2–3-ring OPAHs, three 4-ring OPAHs, two 3-ring PAHs, four 4-ring PAHs, five 5-ring PAHs, and four 6-ring PAHs. Detailed information about these chromophores is listed in Table S4~~3~~. Figure 2 shows the chemical composition of the identified BrC components during the day and night. The total concentration of these chromophores during the day (169.8 ng/m^3) is similar to that at night (171.8 ng/m^3), and the chemical composition of the BrC subgroups is clearly different between the day and night. For example, nitrocatechols, aromatic alcohols/acids and 2–3-rings OPAHs are the major contributors to the total mass concentration of identified BrC chromophores during the day (accounting for 23.3%, 22.3%, and 16.6%, respectively). These BrC chromophores, however, are the minor components during the night (accounting for 12.1% and 15.6%, and 6.9%, respectively). This result indicates the enhanced formation of these chromophores during the day. On the contrary, the relative contributions of nitrophenols and 4–6-ring PAHs are much lower during the day (15.3% and 15.2%, respectively) than those during the night (35.8% and 24.0%, respectively). During the night, 4-nitrophenol (4NP) contributes 24.4% of the total concentration, followed by 2-methyl-4-nitrophenol, fluoranthene, and chrysene (2M4NP 4.7%,

FLU 4.6%, CHR 4.6%, respectively). The higher contributions of nitrophenols and 4–6-rings PAHs at night are likely caused by enhanced primary emissions (Lin et al., 2020; Chen et al., 2021). Our previous study has found that the emitted organic aerosols from coal combustion had a clearly increase at midnight in Shijiazhuang (Huang et al., 2019; Lin et al., 2020). Thus, the large contribute of nitrophenols and 4–6-rings PAHs to total mass concentration at night that may be impacted by emissions from the coal combustion.

To investigate the source of the BrC chromophores, the mass concentrations (these concentrations of chromophores are OC normalized) of the day and night were compared. The day-to-night ratios of identified BrC compounds in mass concentrations is shown in Figure 3. It can be seen that the average day-to-night ratios of WS-BrC chromophores are 4.87 for quinolines, 3.49 for 2–3-ring OPAHs, 3.47 for nitrocatechols, 0.48 for nitrophenols, and 2.53 for aromatic alcohols/acids, respectively. Previous studies have found that quinolines are important products of fossil fuel combustion, and were used as tracers of the vehicular exhaust (Banerjee and Zare, 2015; Xue et al., 2018; Lyu et al., 2019). Thus, the higher day-to-night ratio of quinolines may be due to increased primary emissions from vehicles during the day. Nitrophenols and vanillin are typical biomass burning tracers for atmospheric aerosols (Harrison et al., 2005; Scaramboni et al., 2015; Huang et al., 2021). Previous studies have identified secondary formation as an important source of phthalic acid (PA) and methyl-nitrocatechols (Chow et al., 2015; Zhang and Hatakeyama, 2016; Liu et al., 2017). In this study, vanillin, phthalic acid, and three methyl-nitrocatechols (including 4M5NC, 3M6NC, and 3M5NC) isomers have high day-to-night ratios (4.16, 3.75 and 3.28, respectively). The high day-to-night ratios of these BrC chromophores suggest that biomass burning and secondary formation likely play important roles in the daytime source of BrC.

~~Both nitrophenols and nitrocatechols can be emitted from biomass burning, while their daily variation has surprising differences in this study. Different from the nitrocatechols, However,~~ ~~t~~The average day-to-night ratio (~0.48) of nitrophenols is smaller than one, and this result. ~~The day-to-night ratio of nitrophenols~~ is similar to ~~values in~~ previous studies (Yuan et al., 2016; Schnitzler and Abbatt, 2018). ~~Besides, p~~Previous studies found that emissions from residential coal-fired heating are significant sources of nitrophenols (Wang et al., 2018; Lu et al., 2019).

Although both nitrophenols and nitrocatechols can be emitted from biomass burning, they show largely different day-night variation patterns. The higher concentrations of nitrocatechols during daytime indicate enhanced secondary formation, which is similar to the results observed in urban Beijing (Cheng et al., 2021). In addition, previous studies found that emissions from residential coal-fired heating are significant sources of nitrophenols (Wang et al., 2018; Lu et al., 2019). The higher concentrations of nitrophenols during nighttime, however, suggest that they are mainly emitted from primary emission sources such as residential heating during winter in North China.~~This suggests that coal combustion emissions have important effect on the nocturnal concentration of nitrophenols. Furthermore, Cheng et al. (2021) also reported a different source mechanism for nitrocatechols and nitrophenols. The nitrocatechols peaked at noon, while the nitrophenols peaked in the evening. Their results indicated that the decrease in nitrocatechols was associated with an increase in NO_2 concentration at night. In this study, we also observed an increase in NO_2 concentration at night (see Figure S3), which is similar to the results of Cheng et al. (2021).~~ Compared with the WS-BrC chromophores (the day-to-night ratio > 2.53), the day-to-night ratios of the WIS-BrC chromophores approach or below one, with average ratios of 1.46 for 3-ring PAHs, 1.34 for 4-ring OPAHs, 0.74 for 4-ring PAHs, 0.91 for 5-ring PAHs, and 0.79 for 6-ring PAHs, respectively. A number of studies showed that coal combustion was the dominant source of PAHs (Wang et al., 2018; Xie et al., 2019; Yuan et al., 2020). Thus, the local emissions may be responsible for the majority of 4–6-rings PAHs during the night.

Figure S21~~ (see Supplemental Information)~~ shows the light absorption contributions of the BrC subgroups to total BrC subgroups in the wavelength range between 300 and 420 nm (the absorptions above 420 nm are too low to exactly estimate the contributions), exhibiting large day-night difference. For example, quinolines show evident absorption below 340 nm (3.6% at 310 nm during the day), but negligible contribution above 360 nm. Nitrophenols exhibit a maximum contribution at about 350 nm, while nitrocatechols show higher absorption in the wavelength range from 360 to 400 nm. For PAHs, the absorption maxima shift to a longer wavelength with the increase of the aromatic rings (e.g., 320 nm for 4-ring PAHs and 400 nm for 6-ring PAHs). Overall, the combined light absorption contributions of nitrophenols,

nitrocatechols, and PAHs are 86.5% and 80.1% (averaged between 300 and 420 nm) at night and day, respectively. This result is similar to previous studies, in which PAHs and nitro aromatic compounds were identified as the major chromophores (Huang et al., 2020; Yuan et al., 2020).

The light absorption contribution of these BrC subgroups exhibits obvious day-night differences. For example, the absorption contribution of 2–3-rings OPAHs and nitrocatechols at 365 nm increased by ~2.0 and ~3.5 times during the day compared to that during the night (see Figure S3~~2~~). This result differs from previous studies (Kampf et al., 2012; Gao et al., 2022), which indicated that light absorption of BrC compounds were enhanced after exposure to photo-oxidation. On the other hand, the absorption contributions of nitrophenols and 4–6-rings PAHs at 365 nm are ~1.6 times and ~2.2 times higher at night than at day, respectively. The day-night difference of light absorption of nitrophenols is comparable with previous studies (Harrison et al., 2005; Wang et al., 2020). High absorbance of nitrophenols at night is closely related to their higher mass fraction at night. The absorption characteristics of 4–6-ring PAHs are significantly different from the nitro-phenols, and their absorption per unit mass is larger than that of nitro-phenols. The per unit mass absorbance of PAHs much higher than the low-ring aromatic hydrocarbons (e.g., aromatic alcohols/acids) are due to their strongly conjugated systems. It is worth noting that the absorption contributions of some BrC compounds (including quinolines, aromatic alcohols/acids, 4-ring OPAHs, 3-ring PAHs four subgroups) are much lower than those of the above-mentioned BrC compounds because of their lower mass concentration or light absorption coefficient.

3.3 Comparisons between the low and high pollution period.

The relative contributions of day-night subgroups of BrC chromophores in light absorption and mass concentration were further investigated for different pollution levels. The sampling campaign was classified into low-pollution period ($PM_{2.5}$ < 150 μg m^{-3}) and high-pollution period ($PM_{2.5}$ > 250 μg m^{-3}). Figure 4 (a) shows the mass fractional contributions of the identified subgroups during these periods, which show an evidently different during the day and night. For example, the mass fraction of quinolines during the day (~24.1%) is much higher than during the night (3.4%) at low-pollution period, which may be related to increased vehicle

emissions at day (Rogge et al., 1993; Lyu et al., 2019). Moreover, during the low-pollution period, with good atmospheric dispersion conditions during the day, the fractional concentration of BrC is only 56.9 ng m^{-3} much lower than the nights and high-pollution periods. In the high-pollution period, however, the mass concentration of quinolines is much lower than other BrC chromophores and there is no evident difference between day and night. The mass fraction of aromatic alcohols/acids during the day (35.4%) is much higher than during the night (12.0%) at low-pollution period. For high-pollution period, the mass fraction of aromatic alcohols/acids shows little difference between the day and night. However, their mass concentration during the day (55.5 ng m^{-3}) is higher than that during the night (31.9 ng m^{-3}). Thereinto, the mass concentration of phthalic acid (a tracer from photochemical oxidation) contributes more than 60% to the aromatic alcohols/acids at day for low and high-pollution period (Zhang and Hatakeyama, 2016). This evidence may be suggesting that there is stronger photo-chemical oxidation for aromatic alcohols/acids during the day, especially at low-pollution period.

The mass fractional contribution of nitrocatechols is lower during the day than the night at low-pollution period, while there is obvious secondary formation during the day for high-pollution period. This likely suggests that the daytime conditions of the high-pollution period are inducive for the generation of nitrocatechols. The mass fractional contribution of PAHs during the day is much lower than the night at low-pollution period. At night, residential coal heating is an important source of PAHs, and therefore the daytime contributions of PAHs are much lower than nighttime (Wang et al., 2017; Ni et al., 2021). While there is no day-night difference for PAHs at high-pollution period, which is related to the stable sources and stagnant weather conditions (Huang et al., 2019; Lin et al., 2020). It is noteworthy that the mass contributions of the nitrophenols (nighttime is 2–3 times more than daytime) and 2–3-rings OPAHs (daytime is ~2 times more than nighttime) is opposite between the day and night. This demonstrates that they have stable sources compared to other BrC subgroups even during the low-pollution period and high-pollution period. The higher mass fractional contribution of 2–3-rings OPAHs during the day is related to photochemical oxidation. Nitrophenols exhibit a higher mass fractional contribution during the night than the day, indicating a significant contribution from primary emissions (Lu et al., 2019; Lin et al., 2020). Besides, previous

384 investigations have shown that NO_x concentrations and relative humidity are higher at night in
385 Shijiazhuang, which may have accelerated the formation of nitrophenols in the dark (Yuan et
386 al., 2016; Huang et al., 2019). This result exhibits a clear day-night difference during the low-
387 pollution period than high-pollution period, which indicates that the low-pollution period is
388 easily influenced by the external environment (e.g., solar radiation and wind speed).

389 The day-night light absorption contribution of WS-BrC and WIS-BrC chromophores in
390 different pollution periods is shown in Figure 4 (b). For the low-pollution period, the light
391 absorption contribution of the ten BrC subgroups shows a large difference during the day and
392 night. Thereinto, the WS-BrC chromophores (e.g., quinolines, nitrophenols and nitrocatechols)
393 is the main contributor (accounting for ~75% at 365 nm) of total identified BrC during the day.
394 While, the WIS-BrC chromophores (e.g., 4–6-rings PAHs) become an abundance contributor
395 (accounting for ~65% at 365 nm) during the night. There is an obvious day-night differences in
396 light absorption at low-pollution period, which is consistent with the difference in their mass
397 concentration contribution. Different from the low-pollution period, the light absorption
398 contribution of the total WS-BrC and WIS-BrC chromophores showed no significant day-night
399 differences during the high-pollution period. However, the absorption contributions of
400 subgroups in WS-BrC chromophores have a significant day-night difference (e.g., nitrocatechol
401 and nitrophenols) during the high-pollution period, which is due to the change of the mass
402 contributions. WS-BrC chromophores have stronger light absorption both during the day and
403 night compared to the WIS-BrC chromophores at high pollution period. Specifically, the
404 absorption contribution of nitrocatechols and nitrophenols combined accounts for 66.1% at day
405 and 60.7% at night at 365 nm, respectively, which depend on the different emission sources or
406 formation mechanisms between during the day and night. Our results show a significant day-
407 night differences in mass contributions and absorption contributions of BrC components at
408 different pollution levels. This suggests that the variation of BrC chromophores in different
409 pollution periods may be caused by different sources and weather conditions.

410 **4 Conclusions**

411 In general, our study shows the large day-night differences in optical properties and
412 chemical composition of the bulk BrC in urban atmosphere. Thereinto, WS-BrC is the main

light-absorbing contributors during the day, while WIS-BrC is main light-absorbing compound at night. The polar WS-BrC has higher MAE_{365} compared to the less-polar WIS-BrC, mainly due to the different conjugate systems and functional groups in the two fractions. ~~During the day, polar components such as nitroaromatic have a higher absorption percentage and lower MAE, while non-polar components such as PAHs have a higher absorption percentage and higher MAE during the night.~~ Different types of the identified BrC chromophores exhibit unique characteristics of day-night differences, reflecting their particular sources and formation pathways. For example, nitrocatechols and 2–3-rings OPAHs are important contributors to mass concentration and light absorption during the day, while 4–6-rings PAHs and nitrophenols become the significant contributors at night.

Day-night differences of BrC chromophores are associated with different sources during day (mainly secondary formation and vehicle emission) and night (mainly emissions from residential heating) as well as the dynamic development of planetary boundary layer height~~Day-night differences of BrC chromophores are associated with different sources during day (more secondary formation and vehicle emission) and night (more primary sources such as residential heatingemissions)~~. ~~–~~Moreover, these day-night differences are largely affected by the air pollution level, which determines the concentrations of BrC precursors (e.g., aromatic hydrocarbon and phenols) and oxidants (e.g., NO_x, $NO_3^{\cdot}$ and OH), as well as meteorological conditions (e.g., solar irradiation and RH) (Liu et al., 2012; Laskin et al., 2015; Wang et al., 2019). For example, our results found that the day-night difference of BrC fractions is more pronounced in chemical composition and light absorption during the low-pollution period than high-pollution period. These factors may show different effects on the formation and photobleaching of different types of the identified chromophores. However, our current understanding of the formation mechanisms of and influencing factors on these identified chromophores is still incomplete (Huang et al., 2018; Yuan et al., 2020). Therefore, a combination of more laboratory and field studies is needed to (1) make comprehensive characterization of the chromophore composition BrC in ambient aerosol; (2) explore thoroughly the formation mechanisms of different types of BrC chromophore. This will significantly enhance our understanding of atmospheric BrC formation mechanisms and

442 therefore improve the accuracy of the atmospheric effects of BrC in air quality and climate
443 models.

Data availability. Detailed data can be obtained from https://doi.org/10.5281/zenodo.7690230.

Author contributions. Ru-jin Huang designed the study. Data analysis was done by Yuquan Gong and Rujin Huang. Yuquan Gong and Rujin Huang interpreted data, prepared the display items and wrote the manuscript. Lu Yang, Ting Wang, Wei Yuan, Wei Xu, Wenjuan Cao, Yang Wang, and Yongjie Li commented on and discussed the manuscript.

Competing interests. The authors declare that they have no conflict of interest.

Acknowledgements. We are very grateful to the National Natural Science Foundation of China (NSFC) (No. 41925015), the Strategic Priority Research Program of Chinese Academy of Sciences (No. XDB40000000), the Chinese Academy of Sciences (No. ZDBS-LY-DQC001), and the Cross Innovative Team fund from the State Key Laboratory of Loess and Quaternary Geology (No. SKLLQGTD1801) supported this study.

Financial support. This work was supported by the National Natural Science Foundation of China (NSFC) under Grant No. 41925015, the Strategic Priority Research Program of Chinese Academy of Sciences (No. XDB40000000), the Chinese Academy of Sciences (No. ZDBS-LY-DQC001), and the Cross Innovative Team fund from the State Key Laboratory of Loess and Quaternary Geology (No. SKLLQGTD1801).

References

Alcanzare, R. J. C.: Polycyclic aromatic compounds in wood soot extracts from Henan, China, 2006.

Banerjee, S. and Zare, R. N.: Syntheses of isoquinoline and substituted quinolines in charged microdroplets, Angew. Chem., 127, 15008-15012, 2015.

Chen, L.-W. A., Chow, J. C., Wang, X., Cao, J., Mao, J., and Watson, J. G.: Brownness of Organic Aerosol over the United States: Evidence for Seasonal Biomass Burning and Photobleaching Effects, Environ. Sci. Technol., 55, 8561-8572, 10.1021/acs.est.0c08706, 2021.

Chen, Y. and Bond, T. C.: Light absorption by organic carbon from wood combustion, Atmos. Chem. Phys., 10, 1773-1787, 10.5194/acp-10-1773-2010, 2010.

Cheng, Y., He, K.-b., Du, Z.-y., Engling, G., Liu, J.-m., Ma, Y.-l., Zheng, M., and Weber, R. J.: The characteristics of brown carbon aerosol during winter in Beijing, Atmos. Environ., 127, 355-364, 10.1016/j.atmosenv.2015.12.035, 2016.

Cheng, X., Chen, Q., Li, Y., Huang, G., Liu, Y., Lu, S., Zheng, Y., Qiu, W., Lu, K., Qiu, X., Bianchi, F., Yan, C., Yuan, B., Shao, M., Wang, Z., Canagaratna, M. R., Zhu, T., Wu, Y., and Zeng, L.: Secondary Production of Gaseous Nitrated Phenols in Polluted Urban Environments, Environ. Sci. Technol., 55, 4410-4419, 10.1021/acs.est.0c07988, 2021.

Chow, J. C., Watson, J. G., Robles, J., Wang, X., Chen, L.-W. A., Trimble, D. L., Kohl, S. D., Tropp, R. J., and Fung, K. K.: Quality assurance and quality control for thermal/optical analysis of aerosol samples for organic and elemental carbon, Anal. Bioanal. Chem., 401, 3141-3152, 2011.

Chow, K. S., Huang, X. H., and Yu, J. Z.: Quantification of nitroaromatic compounds in atmospheric fine particulate matter in Hong Kong over 3 years: field measurement evidence for secondary formation derived from biomass burning emissions, Environ.Chem., 13, 665-673, 2015.

Dat, N. D. and Chang, M. B.: Review on characteristics of PAHs in atmosphere, anthropogenic sources and control technologies, Sci Total Environ., 609, 682-693, 10.1016/j.scitotenv.2017.07.204, 2017.

Deng, J., Ma, H., Wang, X., Zhong, S., Zhang, Z., Zhu, J., Fan, Y., Hu, W., Wu, L., Li, X., Ren, L., Pavuluri, C. M., Pan, X., Sun, Y., Wang, Z., Kawamura, K., and Fu, P.: Measurement report: Optical properties and sources of water-soluble brown carbon in Tianjin, North China – insights from organic molecular compositions, Atmos. Chem. Phys., 22, 6449-6470, 10.5194/acp-22-6449-2022, 2022.

Gao, Y., Wang, Q., Li, L., Dai, W., Yu, J., Ding, L., Li, J., Xin, B., Ran, W., and Han, Y.: Optical properties of mountain primary and secondary brown carbon aerosols in summertime, Sci Total Environ., 806, 150570, 2022.

Hammer, M. S., Martin, R. V., van Donkelaar, A., Buchard, V., Torres, O., Ridley, D. A., and Spurr, R. J. D.: Interpreting the ultraviolet aerosol index observed with the OMI satellite instrument to understand absorption by organic aerosols: implications for atmospheric oxidation and direct radiative effects, Atmos. Chem. Phys., 16, 2507-2523, 10.5194/acp-16-2507-2016, 2016.

Harrison, M. A., Barra, S., Borghesi, D., Vione, D., Arsene, C., and Olariu, R. I.: Nitrated phenols in the atmosphere: a review, Atmos. Environ., 39, 231-248, 2005.

Hems, R. F. and Abbatt, J. P. D.: Aqueous Phase Photo-oxidation of Brown Carbon Nitrophenols: Reaction Kinetics, Mechanism, and Evolution of Light Absorption, ACS Earth Space Chem., 2, 225-234, 10.1021/acsearthspacechem.7b00123, 2018.

Hecobian, A., Zhang, X., Zheng, M., Frank, N., Edgerton, E. S., and Weber, R. J.: Water-Soluble Organic Aerosol material and the light-absorption characteristics of aqueous extracts measured

504 over the Southeastern United States, Atmos. Chem. Phys., 10, 5965-5977, 2010.
505 Huang, R.-J., Wang, Y., Cao, J., Lin, C., Duan, J., Chen, Q., Li, Y., Gu, Y., Yan, J., and Xu, W.:
506 Primary emissions versus secondary formation of fine particulate matter in the most polluted city
507 (Shijiazhuang) in North China, Atmos. Chem. Phys., 19, 2283-2298, 2019.
508 Huang, R.-J., Yang, L., Cao, J., Chen, Y., Chen, Q., Li, Y., Duan, J., Zhu, C., Dai, W., and Wang, K.:
509 Brown carbon aerosol in urban Xi'an, Northwest China: the composition and light absorption
510 properties, Environ. Sci. Technol., 52, 6825-6833, 2018.
511 Huang, R.-J., Yang, L., Shen, J., Yuan, W., Gong, Y., Ni, H., Duan, J., Yan, J., Huang, H., and You,
512 Q.: Chromophoric Fingerprinting of Brown Carbon from Residential Biomass Burning, Environ.
513 Sci. Technol. Lett., 2021.
514 Huang, R.-J., Zhang, Y., Bozzetti, C., Ho, K.-F., Cao, J.-J., Han, Y., Daellenbach, K. R., Slowik, J.
515 G., Platt, S. M., and Canonaco, F.: High secondary aerosol contribution to particulate pollution
516 during haze events in China, Nature, 514, 218-222, 2014.
517 Huang, R. J., Yang, L., Shen, J., Yuan, W., Gong, Y., Guo, J., Cao, W., Duan, J., Ni, H., Zhu, C., Dai,
518 W., Li, Y., Chen, Y., Chen, Q., Wu, Y., Zhang, R., Dusek, U., O'Dowd, C., and Hoffmann, T.:
519 Water-Insoluble Organics Dominate Brown Carbon in Wintertime Urban Aerosol of China:
520 Chemical Characteristics and Optical Properties, Environ Sci Technol., 54, 7836-7847,
521 10.1021/acs.est.0c01149, 2020.
522 Iinuma, Y., Böge, O., Gräfe, R., and Herrmann, H.: Methyl-nitrocatechols: atmospheric tracer
523 compounds for biomass burning secondary organic aerosols, Environ Sci Technol., 44, 8453-
524 8459, 2010.
525 Kampf, C. J., Jakob, R., and Hoffmann, T.: Identification and characterization of aging products in
526 the glyoxal/ammonium sulfate system–implications for light-absorbing material in atmospheric
527 aerosols, Atmos. Chem. Phys., 12, 6323-6333, 2012.
528 Kasthuriarachchi, N. Y., Rivellini, L. H., Chen, X., Li, Y. J., and Lee, A. K. Y.: Effect of Relative
529 Humidity on Secondary Brown Carbon Formation in Aqueous Droplets, Environ Sci Technol.,
530 54, 13207-13216, 10.1021/acs.est.0c01239, 2020.
531 Kirchstetter, T. W., Novakov, T., and Hobbs, P. V.: Evidence that the spectral dependence of light
532 absorption by aerosols is affected by organic carbon, J Geophys Res-Atmos., 109, 2004.
533 Kitanovski, Z., Grgić, I., Yasmeen, F., Claeys, M., and Čusak, A.: Development of a liquid
534 chromatographic method based on ultraviolet–visible and electrospray ionization mass
535 spectrometric detection for the identification of nitrocatechols and related tracers in biomass
536 burning atmospheric organic aerosol, Rapid Commun Mass Sp., 26, 793-804, 2012.
537 Laskin, A., Laskin, J., and Nizkorodov, S. A.: Chemistry of atmospheric brown carbon, Chem Rev.,
538 115, 4335-4382, 10.1021/cr5006167, 2015.
539 Li, J., Zhang, Q., Wang, G., Li, J., Wu, C., Liu, L., Wang, J., Jiang, W., Li, L., and Ho, K. F.: Optical
540 properties and molecular compositions of water-soluble and water-insoluble brown carbon (BrC)
541 aerosols in northwest China, Atmos. Chem. Phys., 20, 4889-4904, 2020.
542 Li, X., Zhao, Q., Yang, Y., Zhao, Z., Liu, Z., Wen, T., Hu, B., Wang, Y., Wang, L., and Wang, G.:
543 Composition and sources of brown carbon aerosols in megacity Beijing during the winter of 2016,
544 Atmos. Res., 262, 105773, 2021.
545 Lin, C., Huang, R.-J., Xu, W., Duan, J., Zheng, Y., Chen, Q., Hu, W., Li, Y., Ni, H., and Wu, Y.:
546 Comprehensive Source Apportionment of Submicron Aerosol in Shijiazhuang, China: Secondary
547 Aerosol Formation and Holiday Effects, ACS Earth and Space Chem., 4, 947-957, 2020.

Lin, P., Bluvshtein, N., Rudich, Y., Nizkorodov, S. A., Laskin, J., and Laskin, A.: Molecular Chemistry of Atmospheric Brown Carbon Inferred from a Nationwide Biomass Burning Event, Environ. Sci. Technol., 51, 11561-11570, 10.1021/acs.est.7b02276, 2017.

Lin, P., Rincon, A. G., Kalberer, M., and Yu, J. Z.: Elemental Composition of HULIS in the Pearl River Delta Region, China: Results Inferred from Positive and Negative Electrospray High Resolution Mass Spectrometric Data, Environ. Sci. Technol., 46, 7454-7462, 2012.

Liu, S., Shilling, J. E., Song, C., Hiranuma, N., Zaveri, R. A., and Russell, L. M.: Hydrolysis of organonitrate functional groups in aerosol particles, Aerosol. Sci. Technol., 46, 1359-1369, 2012.

Liu, J., Lin, P., Laskin, A., Laskin, J., Kathmann, S. M., Wise, M., Caylor, R., Imholt, F., Selimovic, V., and Shilling, J. E.: Optical properties and aging of light-absorbing secondary organic aerosol, Atmos. Chem. Phys., 16, 12815-12827, 10.5194/acp-16-12815-2016, 2016.

Liu, W.-J., Li, W.-W., Jiang, H., and Yu, H.-Q.: Fates of chemical elements in biomass during its pyrolysis, Chem. Rev., 117, 6367-6398, 2017.

Lu, C., Wang, X., Li, R., Gu, R., Zhang, Y., Li, W., Gao, R., Chen, B., Xue, L., and Wang, W.: Emissions of fine particulate nitrated phenols from residential coal combustion in China, Atmos. Environ., 203, 10-17, https://doi.org/10.1016/j.atmosenv.2019.01.047, 2019.

Lyu, R., Shi, Z., Alam, M. S., Wu, X., Liu, D., Vu, T. V., Stark, C., Fu, P., Feng, Y., and Harrison, R. M.: Insight into the composition of organic compounds (≥ C 6) in PM 2.5 in wintertime in Beijing, China, Atmos. Chem. Phys., 19, 10865-10881, 2019.

Ni, H., Huang, R.-J., Pieber, S. M., Corbin, J. C., Stefenelli, G., Pospisilova, V., Klein, F., Gysel-Beer, M., Yang, L., and Baltensperger, U.: Brown carbon in primary and aged coal combustion emission, Environ. Sci. Technol., 55, 5701-5710, 2021.

Rogge, W. F., Hildemann, L. M., Mazurek, M. A., Cass, G. R., and Simoneit, B. R.: Sources of fine organic aerosol. 2. Noncatalyst and catalyst-equipped automobiles and heavy-duty diesel trucks, Environ. Sci. Technol., 27, 636-651, 1993.

Scaramboni, C., Urban, R. C., Lima-Souza, M., Nogueira, R. F. P., Cardoso, A. A., Allen, A. G., and Campos, M. d. M.: Total sugars in atmospheric aerosols: An alternative tracer for biomass burning, Atmos. Environ., 100, 185-192, 2015.

Schnitzler, E. G. and Abbatt, J. P.: Heterogeneous OH oxidation of secondary brown carbon aerosol, Atmos. Chem. Phys., 18, 14539-14553, 2018.

Shen, R., Liu, Z., Chen, X., Wang, Y., Wang, L., Liu, Y., and Li, X.: Atmospheric levels, variations, sources and health risk of PM2. 5-bound polycyclic aromatic hydrocarbons during winter over the North China Plain, Sci. Total Environ., 655, 581-590, 2019.

Siemens, K., Morales, A., He, Q., Li, C., Hettiyadura, A. P., Rudich, Y., and Laskin, A.: Molecular Analysis of Secondary Brown Carbon Produced from the Photooxidation of Naphthalene, Environ. Sci. Technol., 56, 3340-3353, 2022.

Teich, M., van Pinxteren, D., Wang, M., Kecorius, S., Wang, Z., Müller, T., Močnik, G., and Herrmann, H.: Contributions of nitrated aromatic compounds to the light absorption of water-soluble and particulate brown carbon in different atmospheric environments in Germany and China, Atmos. Chem. Phys., 17, 1653-1672, 2017.

Wang, H., Gao, Y., Wang, S., Wu, X., Liu, Y., Li, X., Huang, D., Lou, S., Wu, Z., and Guo, S.: Atmospheric processing of nitrophenols and nitrocresols from biomass burning emissions, J. Geophys.Res. Atmos., 125, e2020JD033401, 2020.

Wang, L., Wang, X., Gu, R., Wang, H., Yao, L., Wen, L., Zhu, F., Wang, W., Xue, L., Yang, L., Lu,

592 K., Chen, J., Wang, T., Zhang, Y., and Wang, W.: Observations of fine particulate nitrated phenols
593 in four sites in northern China: concentrations, source apportionment, and secondary formation,
594 Atmos. Chem. Phys., 18, 4349-4359, 10.5194/acp-18-4349-2018, 2018.
595 Wang, Q., Han, Y., Ye, J., Liu, S., Pongpiachan, S., Zhang, N., Han, Y., Tian, J., Wu, C., and Long,
596 X.: High contribution of secondary brown carbon to aerosol light absorption in the southeastern
597 margin of Tibetan Plateau, Geophys.Res. Lett., 46, 4962-4970, 2019a.
598 Wang, X., Gu, R., Wang, L., Xu, W., Zhang, Y., Chen, B., Li, W., Xue, L., Chen, J., and Wang, W.:
599 Emissions of fine particulate nitrated phenols from the burning of five common types of biomass,
600 Environ Pollut., 230, 405-412, 10.1016/j.envpol.2017.06.072, 2017.
601 Wang, Y., Hu, M., Wang, Y., Zheng, J., Shang, D., Yang, Y., Liu, Y., Li, X., Tang, R., and Zhu, W.:
602 The formation of nitro-aromatic compounds under high NO x and anthropogenic VOC conditions
603 in urban Beijing, China, Atmos. Chem. Phys., 19, 7649-7665, 2019b.
604 Xie, C., Xu, W., Wang, J., Wang, Q., Liu, D., Tang, G., Chen, P., Du, W., Zhao, J., and Zhang, Y.:
605 Vertical characterization of aerosol optical properties and brown carbon in winter in urban Beijing,
606 China, Atmos. Chem. Phys., 19, 165-179, 2019.
607 Xue, X., Zeng, M., and Wang, Y.: Highly active and recyclable Pt nanocatalyst for hydrogenation
608 of quinolines and isoquinolines, Applied Catalysis A: General., 560, 37-41, 2018.
609 Yuan, B., Liggio, J., Wentzell, J., Li, S.-M., Stark, H., Roberts, J. M., Gilman, J., Lerner, B., Warneke,
610 C., and Li, R.: Secondary formation of nitrated phenols: insights from observations during the
611 Uintah Basin Winter Ozone Study (UBWOS) 2014, Atmos. Chem. Phys., 16, 2139-2153, 2016.
612 Yuan, W., Huang, R.-J., Yang, L., Guo, J., Chen, Z., Duan, J., Wang, T., Ni, H., Han, Y., and Li, Y.:
613 Characterization of the light-absorbing properties, chromophore composition and sources of
614 brown carbon aerosol in Xi'an, northwestern China, Atmos. Chem. Phys., 20, 5129-5144, 2020.
615 Yuan, W., Huang, R.-J., Yang, L., Wang, T., Duan, J., Guo, J., Ni, H., Chen, Y., Chen, Q., and Li, Y.:
616 Measurement report: PM 2.5-bound nitrated aromatic compounds in Xi'an, Northwest China–
617 seasonal variations and contributions to optical properties of brown carbon, Atmos. Chem. Phys.,
618 21, 3685-3697, 2021.
619 Zhan, Y., Li, J., Tsona, N. T., Chen, B., Yan, C., George, C., and Du, L.: Seasonal variation of water-
620 soluble brown carbon in Qingdao, China: Impacts from marine and terrestrial emissions, Environ.
621 Res., 212, 113144, https://doi.org/10.1016/j.envres.2022.113144, 2022.
622 Zhang, S., Zhang, W., Wang, K., Shen, Y., Hu, L., and Wang, X.: Concentration, distribution and
623 source apportionment of atmospheric polycyclic aromatic hydrocarbons in the southeast suburb
624 of Beijing, China, Environ. Monit. Assess., 151, 197-207, 2009.
625 Zhang, Y. and Hatakeyama, S.: New directions: Need for better understanding of source and
626 formation process of phthalic acid in aerosols as inferred from, Atmos. Environ., 140, 147e149,
627 2016.

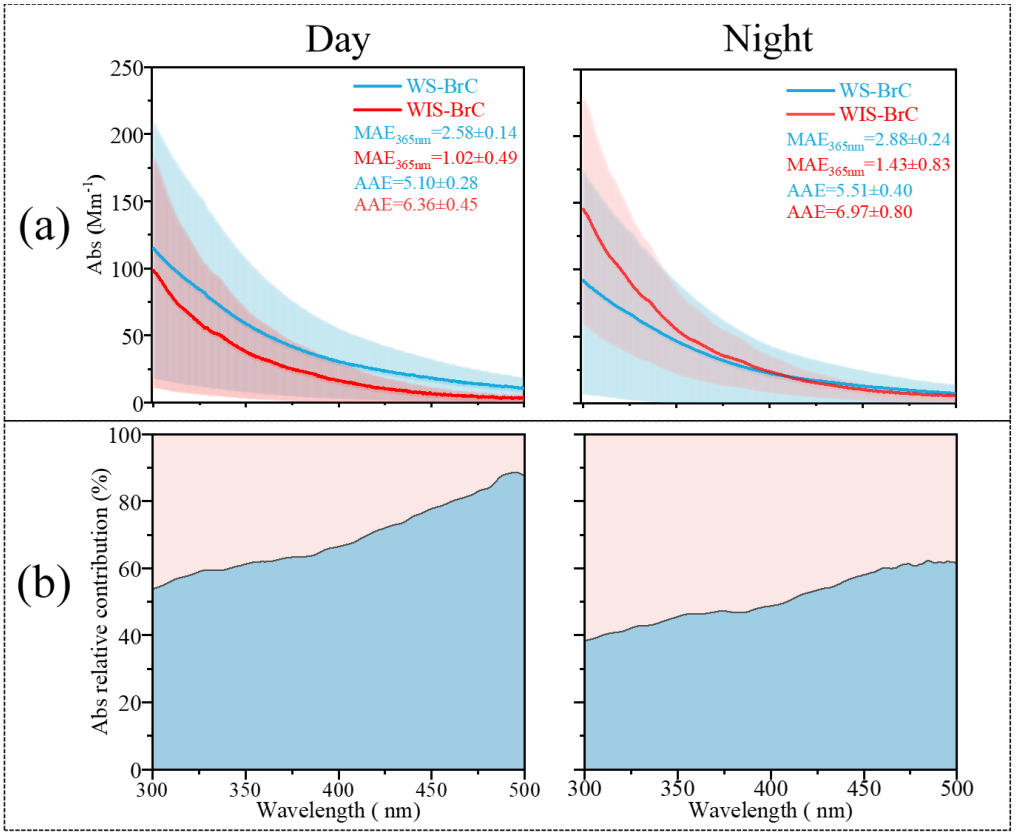

Figure 1. (a) Day-night absorption spectra (Abs, in the wavelength range of 300–500 nm), mass absorption efficiency (MAE, determined at 365 nm), and absorption Ångström exponent (AAE, calculated between 300 and 400 nm) of water-soluble/insoluble BrC (WS-/WIS-BrC) in Shijiazhuang. (b) Light-absorbing proportion of WS-BrC and WIS-BrC between 300 to 500 nm.

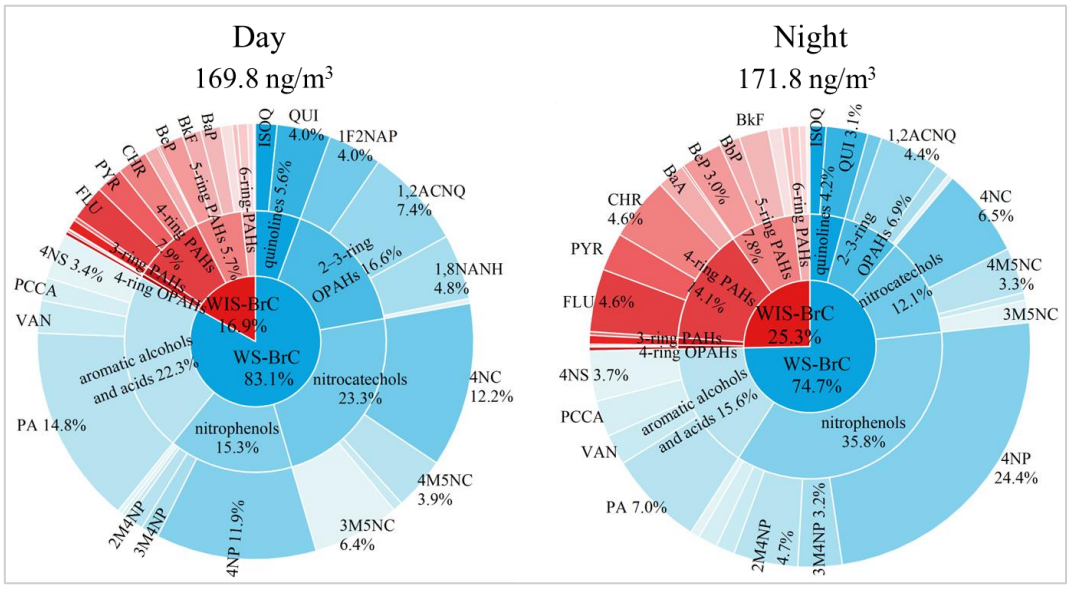

Figure 2. Mass fraction of the identified BrC chromophores during the day and night (details

of the identified BrC chromophores are shown in Table S1).

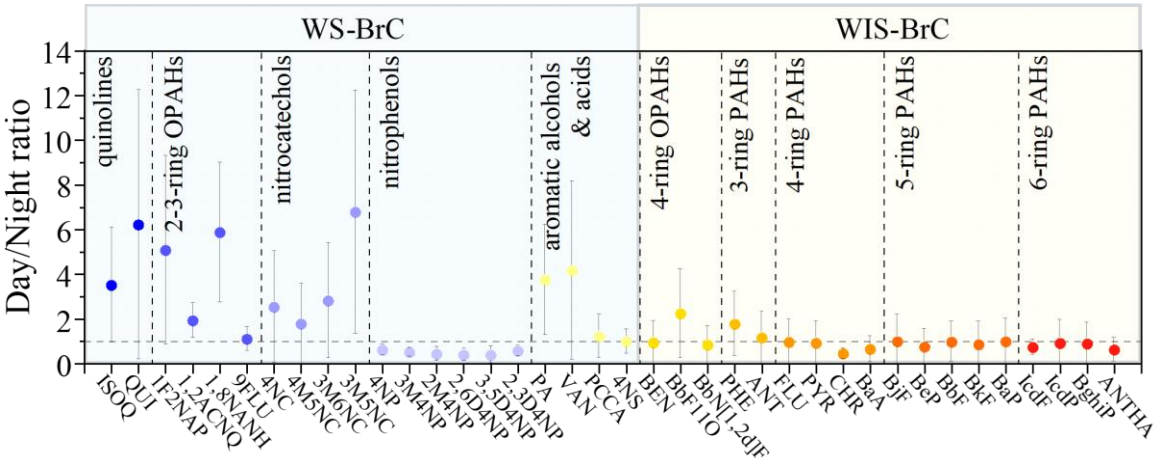

Figure 3. Day-to-night ratios of the concentrations of different BrC chromophores.

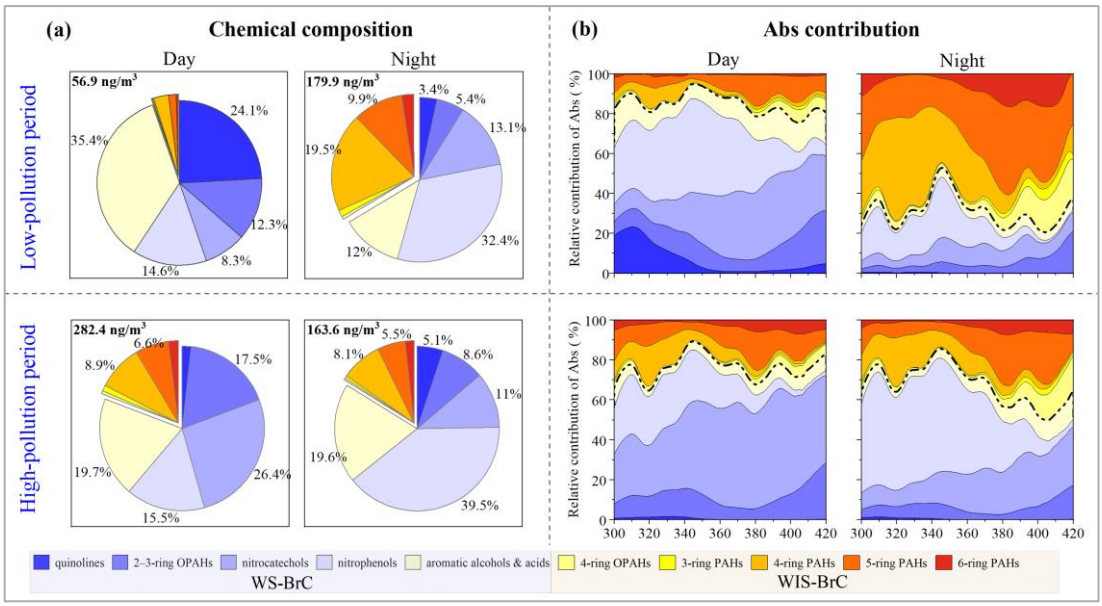

Figure 4. Day-night fractional contributions of mass concentrations **(a)** and light absorption **(b)** of the ten BrC subgroups in low-pollution period and high-pollution period. Here the BrC chromophore is the main chromophore substance that has been identified. In **(b)** WS-BrC is below the dotted line and WIS-BrC is above the dotted line.